aPKC enables development of zonula adherens by antagonizing centripetal contraction of the circumferential actomyosin cables

Masaru Kishikawa, Atsushi Suzuki* and Shigeo Ohno

Department of Molecular Biology, Yokohama City University Graduate School of Medical Science, 3-9 Fuku-ura, Kanazawa-ku, Yokohama, 236-0004, Japan

*Author for correspondence (e-mail: abell@med.yokohama-cu.ac.jp)

Accepted 12 May 2008
Journal of Cell Science 121, 2481-2492 Published by The Company of Biologists 2008
doi:10.1242/jcs.024109

Summary

Atypical protein kinase C (aPKC) generally plays crucial roles in the establishment of cell polarity in various biological contexts. In mammalian epithelial cells, aPKC essentially works towards the transition of primordial spot-like adherens junctions (AJs) into continuous belt-like AJs, also called zonula adherens, lined with perijunctional actin belts. To reveal the mechanism underlying this aPKC function, we investigated the functional relationship between aPKC and myosin II, the essential role of which in epithelial-junction development was recently demonstrated. Despite its deleterious effects on junction formation, overexpression of a dominant-negative mutant of aPKC (aPKCλ kn) did not interfere with the initial phase of myosin-II activation triggered by the formation of Ca^{2+}-switch-induced cell-cell contacts. Furthermore, cells overexpressing aPKCλ kn exhibited myosin-II-dependent asymmetric organization of F-actin along the apicobasal axis, suggesting that aPKC contributes to junction development without affecting the centripetal contraction of the circumferential actomyosin cables. Time-lapse analyses using GFP-actin directly revealed that the circumferential actomyosin cables were centrifugally expanded and developed into perijunctional actin belts during epithelial polarization, and that aPKCλ kn specifically compromised this process. Taken together, we conclude that aPKC is required for antagonizing the myosin-II-driven centripetal contraction of the circumferential actin cables, thereby efficiently coupling the myosin-II activity with junction development and cell polarization. The present results provide novel insights into not only the site of action of aPKC kinase activity but also the role of actomyosin contraction in epithelial polarization.

Supplementary material available online at
http://jcs.biologists.org/cgi/content/full/121/15/2481/DC1

Key words: PAR, aPKC, Actin dynamics, Adherens junction, Epithelial cells, Polarity

Introduction

Epithelial cells develop a set of characteristic cell-cell adhesion structures – termed tight junctions (TJs), belt-like adherens junctions (AJs) and desmosomes – in order to establish and maintain their apicobasal polarity (Yeaman et al., 1999). Among these structures, belt-like AJs, also called zonula adherens, represent the most essential adhesion structures, in which E-cadherin works as an adhesion molecule and to which tangential thick actin belts, called perijunctional actin belts, are closely associated (Tsukita et al., 1992; Yonemura et al., 1995). Owing to their crucial roles in epithelial-cell polarity, the development and regulation of belt-like AJs has been an important research subject in cell biology.

The developmental process of belt-like AJs is tightly coupled with dramatic reorganization of F-actin (Adams et al., 1998; Vaezi et al., 2002; Vasioukhin et al., 2000; Yonemura et al., 1995; Zhang et al., 2005). Initial cell-cell contacts, via cadherin, induce rapid actin polymerization and cadherin clustering, which result in the formation of spot-like AJs, to which multiple actin filaments are perpendicularly associated (hereafter referred to as radial actin fibers; see Fig. 1B) (Adams et al., 1998; Vasioukhin et al., 2000; Yonemura et al., 1995). Spot-like AJs are also formed in fibroblasts. However, the spot-like AJs observed in epithelial cells are very unique because they subsequently become reorganized into continuous belt-like AJs. During this process, the free ends of radial actin fibers associate with the epithelial-specific structure, the circumferential loose cables of F-actin (hereafter referred to as circumferential actin cables; see Fig. 1B), and finally develop into perijunctional actin belts (Vaezi et al., 2002; Vasioukhin et al., 2000). Immunofluorescence studies have demonstrated that, as epithelial cells become polarized, the circumferential actin cables expand towards the cell periphery with concomitant shortening of the radial actin fibers, and finally develop into perijunctional actin belts that are closely associated with the membrane (Yonemura et al., 1995). These results suggest that the epithelium-specific F-actin reorganization is crucial for the formation of belt-like AJs. However, the underlying molecular mechanisms are largely unknown.

The perijunctional actin belts as well as circumferential actin cables contain activated myosin II (Ivanov et al., 2005; Zhang et al., 2005). Furthermore, recent studies have revealed that the addition of myosin-II inhibitors or siRNA-mediated knockdown of nonmuscle myosin heavy chain IIA disrupt the circumferential actin cables and suppress epithelial-junction development and cell polarization (Chen and Macara, 2005; Ivanov et al., 2007; Ivanov et al., 2005; Miyake et al., 2006; Zhang et al., 2005), indicating that myosin-II activity is essential for epithelial-junction development. Taken together with the observation that the

circumferential actin cables exhibit a continuous flux of centripetal (retrograde) movement from the cytoplasmic periphery towards the nucleus when the cells are free from cell-cell contacts (Vaezi et al., 2002), these results suggest that myosin-II-dependent centripetal contraction of the circumferential actin cables is crucial for belt-like AJ formation. However, there are apparently conflicting results that the same myosin inhibitors suppress the junction disassembly (Ivanov et al., 2004). Furthermore, several studies have demonstrated that the circumferential actin cables disassemble in the vicinity of the cell-cell boundary when the cell makes contact with other cells (Adams et al., 1996; Gloushankova et al., 1997; Krendel and Bonder, 1999; Yamada and Nelson, 2007). The authors argued that actomyosin contraction does not act at the region of cell-cell contact but at cell-cell-contact-free areas in order to expand the contact regions laterally and render the contacting cells more compact. Taken together, it still remains to be elucidated how myosin-II-dependent contraction of the circumferential actin cables is used for belt-like AJ formation and epithelial polarization (Mege et al., 2006).

Atypical protein kinase C (aPKC) is a crucial component of the aPKC–PAR-6–PAR-3 complex, an evolutionarily conserved signaling complex for cell polarity (Macara, 2004; Suzuki and Ohno, 2006). In epithelial cells, aPKC plays an essential role in the development of epithelium-specific junction structures, such as belt-like AJs and TJs, and thus contributes to the development of apicobasal polarity (Knust and Bossinger, 2002; Suzuki et al., 2001). By analyzing the repolarization process during wound healing of a mouse epithelial cell line, MTD1-A cells, we previously demonstrated that the kinase activity of aPKC is not required for the formation of spot-like AJs to which aPKC itself is recruited, but is essential for their subsequent transition into belt-like AJs (Suzuki et al., 2002; Suzuki et al., 2001). We further found that cells subjected to aPKC inhibition terminated the F-actin reorganization at an intermediate state in which the radial actin fibers remained associated with the circumferential actin cables perpendicularly. In the present study, we examined the possibility that aPKC contributes to the development of epithelium-specific junctions by regulating myosin-II activity. Our results indicate that aPKC does not affect initial myosin-II activation triggered by Ca^{2+}-switch-induced formation of cell-cell contacts, but is required to antagonize the myosin-II-dependent centripetal contraction of the circumferential actin cables within individual cells. By doing so, aPKC transforms the centripetal contractile force of the circumferential actin cables towards the development of belt-like AJs. The present results provide not only important clues for the molecular basis of how aPKC regulates the development of epithelium-specific junctions but also a novel concept for the role of the contractile force of the perijunctional actin belts.

Results

Two isoforms of mammalian aPKC – aPKCλ and aPKCζ – act redundantly in epithelial-junction development

Previously, we reported that overexpression of aPKCλ kn, a dominant-negative mutant of aPKCλ, blocked junction reformation during the wound-healing process of MTD1-A cells at an intermediate step that displays discontinuous spot-like AJs (Suzuki et al., 2002). In the present study, we confirmed similar effects of aPKCλ kn on the junction reformation induced by a Ca^{2+} switch. Control MTD1-A cells developed continuous belt-like AJs that were aligned with the highly concentrated perijunctional actin belts within 6 hours after Ca^{2+} repletion (Fig. 1A, *lacZ*; supplementary material Fig. S1) (Yonemura et al., 1995). By contrast, the junction development in aPKCλ-kn-overexpressing cells terminated with the exhibition of spot-like AJs that accumulated numerous junction components – such as ZO-1, E-cadherin and occludin – in a mixture (Fig. 1A, aPKCλ kn; M.K. and A.S., unpublished). F-actin reorganization also ended at an intermediate state, in which radial actin fibers (yellow arrowheads in the enlarged merged views in Fig. 1A; Fig. 1B) were tethered to loosely or tightly bundled circumferential actin cables (arrowheads in Fig. 1A; Fig. 1B), with punctate accumulation of F-actin on the spot-like AJs (actin puncta; arrows in Fig. 1A; Fig. 1B) (Nelson, 2003; Vasioukhin et al., 2000; Yonemura et al., 1995; Zhang et al., 2005). Similar phenotypes were observed after aPKC expression was reduced by RNA interference (RNAi) (Fig. 1C,D). Although this method was only applicable to subconfluent cells that did not complete belt-like AJ formation at all cell-cell borders, cells subjected to control RNAi exhibited continuous belt-like AJ formation in ~50% of all cell-cell-contact regions after a Ca^{2+} switch (Fig. 1D, NS). By contrast, double-knockdown of two aPKC isoforms, aPKCλ and aPKCζ, resulted in a blockade of belt-like AJ formation at all cell-cell-contact regions, without any reduction of expression levels of E-cadherin, α-catenin or β-catenin (Fig. 1C,D, λ3+ζ1). Single knockdown of aPKCλ (Fig. 1C,D, λ3) did not exert any detectable effects, indicating that aPKCλ and aPKCζ function redundantly for junction development in MTD1-A cells. These results also established that aPKCλ kn can exert dominant-negative effects on both aPKC isoforms (Suzuki et al., 2001). In the following experiments, we suppressed aPKC activity by overexpressing aPKCλ kn, because this method is easily applicable to confluent monolayers of MTD1-A cells.

Myosin inhibitors and aPKCλ kn block junction development similarly but affect F-actin reorganization differently

Close functional relationships between the aPKC–PAR-6–PAR-3 complex and myosin II have been demonstrated during embryogenesis in *Caenorhabditis elegans* and *Drosophila melanogaster* (Barros et al., 2003; Munro et al., 2004). By contrast, myosin II was recently demonstrated to be required for the development of epithelium-specific continuous junction structures in various epithelial cells (Ivanov et al., 2005; Miyake et al., 2006; Zhang et al., 2005), suggesting the possibility that aPKC promotes junction development by regulating myosin-II activity. As a first step towards assessing this possibility, we compared the effects of myosin-II inhibitors on the junction development of MTD1-A cells with the effects of aPKCλ-kn overexpression. We treated cells with 100 μM blebbistatin (an inhibitor of myosin-II ATPase activity) (Straight et al., 2003) or 20 μM Y27632 (an inhibitor of ROCK, which is essential for myosin light-chain phosphorylation) (Narumiya et al., 2000) for 1 hour in low Ca^{2+} (LC) medium before a Ca^{2+} switch (Fig. 1A, right panels). Consistent with previous results, these pre-treatments commonly blocked the development of spot-like AJs into continuous belt-like AJs and TJs, in a similar manner to aPKCλ-kn overexpression. However, the effects on F-actin reorganization were distinctively different between myosin-II inhibition and aPKCλ-kn overexpression. In contrast to cells overexpressing aPKCλ kn, cells treated with the myosin inhibitors commonly showed loss of the characteristic F-actin organization, such as the circumferential actin cables and radial actin fibers. Treatment with Y27632 also weakened the punctate staining of F-actin on spot-like AJs. Taken together with previous reports that myosin II and ROCK are required for E-cadherin

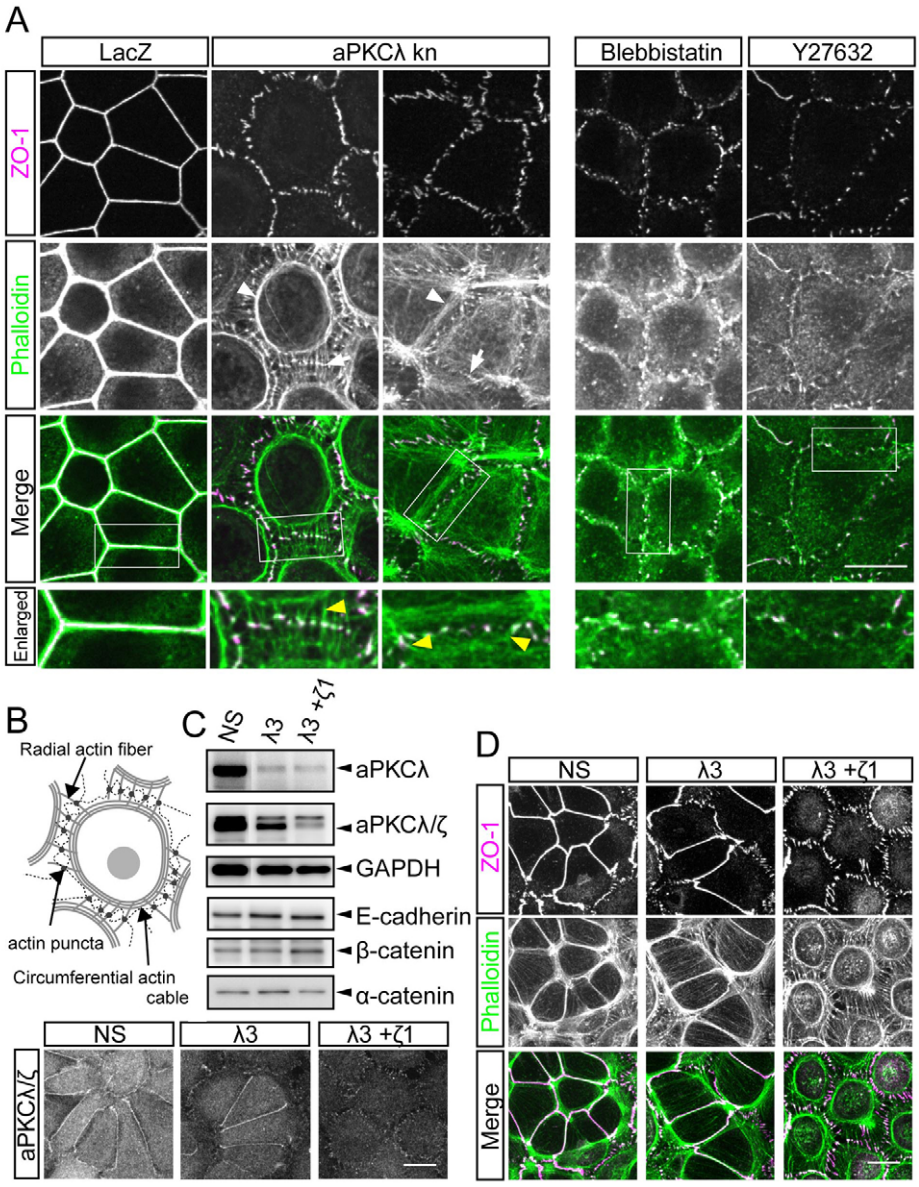

Fig. 1. Comparison of the effects of aPKCλ kn and of myosin-II inhibitors on the junction development of MTD1-A cells. (A) Myosin inhibitors and aPKCλ kn, a dominant-negative mutant of aPKCλ, block junction development similarly but affect actin reorganization differently. Confluent monolayers of MTD1-A cells transformed by adenovirus vectors encoding β-galactosidase (LacZ) or aPKCλ kn were cultured in LC medium for 40 hours and then subjected to a Ca^{2+} switch in the presence or absence of the myosin inhibitors blebbistatin (100 μM) or Y27632 (20 μM). The cells were fixed at 6 hours after the Ca^{2+} switch and stained with an anti-ZO-1 antibody (magenta in merged images) and phalloidin (green in merged images). The images shown are single confocal sections that were selected to demonstrate the ZO-1 staining most clearly. Enlargements of the boxed regions in the merged views are shown at the bottom. For cells overexpressing aPKCλ kn, two typical images are presented, in which the left and right panels show cells exhibiting tightly and loosely bundled circumferential actin cables, respectively (each represents ~40% and ~60% of aPKCλ-kn-overexpressing cells, respectively). White arrowheads, circumferential actin cables; arrows, punctate staining of F-actin on spot-like AJs; yellow arrowheads, radial actin fibers. (B) Schematic presentation of the intermediate state of F-actin organization observed in aPKCλ-kn-overexpressing cells. (C) RNAi knockdown of aPKC isoforms in MTD1-A cells. Subconfluent MTD1-A cells were transfected with the indicated siRNA oligonucleotide duplexes (NS, non-silencing siRNA; λ3, *aPKCλ* siRNA; ζ1, *aPKCζ* siRNA). Top panels: western blot analyses of total extracts of cells subjected to the indicated RNAi. aPKCλ was specifically detected by an anti-aPKCι (human aPKCλ) antibody, whereas both aPKC isoforms (aPKCλ and aPKCζ) were simultaneously detected by an anti-aPKC antibody (C20) that reacts with both isoforms. GAPDH was used as a loading control. The data for E-cadherin, α-catenin and β-catenin indicated no significant change in the expression levels of these AJ proteins. Images shown underneath: the indicated cells were immunostained with an anti-aPKC antibody (C20). (D) aPKC knockdown suppresses junction development after a Ca^{2+} switch, in a similar manner to aPKCλ-kn overexpression. The indicated cells were subjected to a Ca^{2+} switch as described in A and then immunostained with an anti-ZO-1 antibody (magenta in merged images) and phalloidin (green in merged images). Scale bars: 10 μm.

accumulation at initial cell-cell-contact regions and radial actin-fiber formation (Shewan et al., 2005; Vaezi et al., 2002), these results suggest that the myosin inhibitors suppressed F-actin reorganization at an early stage of junction development, when aPKC activity is not required. These findings indicate that, despite their apparently similar effects on junction formation, myosin II functions independently of aPKC, at least at the initial stage of junction development.

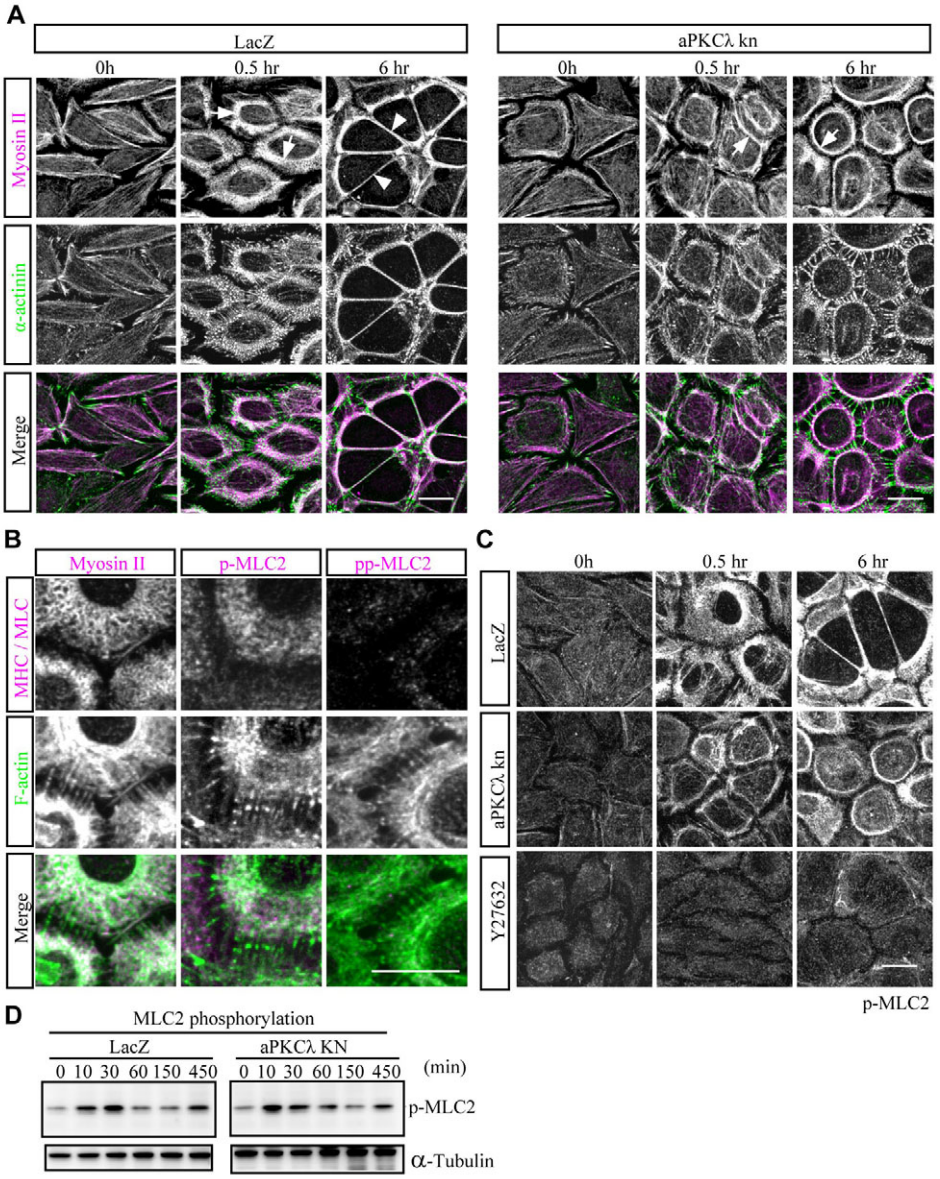

Fig. 2. Suppression of aPKC activity does not affect cell-cell-contact-induced myosin-II activation. (A) MTD1-A cells transfected with adenovirus vectors encoding β-galactosidase (LacZ) or aPKCλ kn were subjected to a Ca^{2+} switch as described in the legend for Fig. 1, fixed at the indicated times after the Ca^{2+} switch, and double stained with a mixture of antibodies against nonmuscle myosin heavy chain IIA and IIB (magenta in merged images) and against α-actinin (green in merged images). Arrows, circumferential actin cables; arrowheads, perijunctional actin belts. (B) Control MTD1A cells were fixed at 30 minutes after a Ca^{2+} switch and double stained for F-actin (phalloidin; green in merged images) and with antibodies against either myosin II, Ser19 monophosphorylated myosin light-chain 2 (p-MLC2) or Thr18 and Ser19 diphosphorylated MLC2 (pp-MLC2) (magenta in merged images) as indicated at the top. Note that radial actin fibers were free from myosin II. (C) MTD1-A cells were immunostained with anti-p-MLC2 antibody at the indicated times after the Ca^{2+} switch. Pre-treatment with Y27632 completely abolishes the staining, suggesting that ROCK is dominantly responsible for this phosphorylation. (D) Total cell extracts of MTD1-A cells were prepared at the indicated times after the Ca^{2+} switch, and the changes in the p-MLC2 level were analyzed by western blotting. Note that overexpression of aPKCλ kn does not affect the Ca^{2+}-switch-induced increase in p-MLC2. Scale bars: 10 μm.

aPKCλ kn does not affect Ca^{2+}-switch-induced activation of myosin II in the early stage of junction formation

Next, we analyzed myosin-II localization and activation in polarizing MTD1A cells, and examined the effects of aPKCλ on these activities. Because MTD1-A cells dominantly express nonmuscle myosin heavy chains IIA and IIB (M.K. and A.S., unpublished), we stained these chains using a mixture of specific antibodies that recognize these isoforms. In control cells expressing *lacZ*, myosin II showed weak peripheral localization in depolarized cells (Fig. 2A). Upon Ca^{2+} repletion, it immediately accumulated on loosely bundled circumferential actin cables (Fig. 2A, arrows, 0.5 hours). Because the cables contained Ser19 monophosphorylated regulatory myosin light chain (p-MLC2) (Fig. 2B,C), these circumferential actin cables were considered to be contractile actomyosin bundles. By contrast, radial actin fibers, which were strongly positive for α-actinin (Fig. 2A), were almost completely free from myosin II (Vaezi et al., 2002) (Fig. 2B), suggesting that radial actin fibers are not contractile structures. In the later stage, the circumferential actin cables progressively developed into highly compacted perijunctional actin belts that were in close contact with cell-cell contacts and remained positive for p-MLC2 (arrowheads in Fig. 2A, 6 hours; Fig. 2C, 6 hours; supplementary material Fig. S2). Western blot analysis of p-MLC2 in total cell lysate also revealed the rapid increase in the level of p-MLC2 upon Ca^{2+}-switch-induced cell-cell contact, although the time courses of bulk MLC2 phosphorylation did not appear to be perfectly consistent with the immunocytochemical results containing spatiotemporal information: bulk MLC2 phosphorylation initially peaked at the very early stage after a Ca^{2+} switch (30 minutes) and showed a slight increase again at 7.5 hours when the cells completed the formation of belt-like AJs and TJs. Notably, aPKCλ-kn overexpression did not inhibit the accumulation of myosin II and p-MLC2 on the circumferential actin cables (arrows in Fig. 2A; Fig. 2C) or affect the level and time course of MLC2 monophosphorylation (Fig. 2D). Nevertheless, most of the circumferential actomyosin cables in aPKCλ-kn-overexpressing cells were not expanded or brought into close contact with the plasma membrane, even at 6 hours after the Ca^{2+} switch (Fig. 2A,C).

Ivanov et al. demonstrated a transient increase of Thr18 and Ser19 diphosphorylated MLC2 (pp-MLC2) 1 hour after Ca^{2+} repletion in T84 cells (Ivanov et al., 2005). However, we could not detect such an early increase in the level of pp-MLC2 in MTD1-A cells not only biochemically but also immunocytochemically (Fig. 2B; supplementary material Fig. S2). This discrepancy might arise from cell-type difference. However, Ivanov et al. and we both found that pp-MLC2 was exclusively detected on the matured perijunctional actin belts, but not on the circumferential actin cables (supplementary material Fig. S2) (Ivanov et al., 2005), suggesting that pp-MLC2 is involved in the final stage of junctional development, when the maturation of perijunctional actin belts proceeds, but not in the early stage, when the circumferential actin cable vigorously develops and starts to expand. Consistently, this increase of pp-MLC2 at the final stage of junctional development was suppressed in aPKCλ-kn-overexpressing cells, in which the completion of perijunctional actin belts was significantly inhibited.

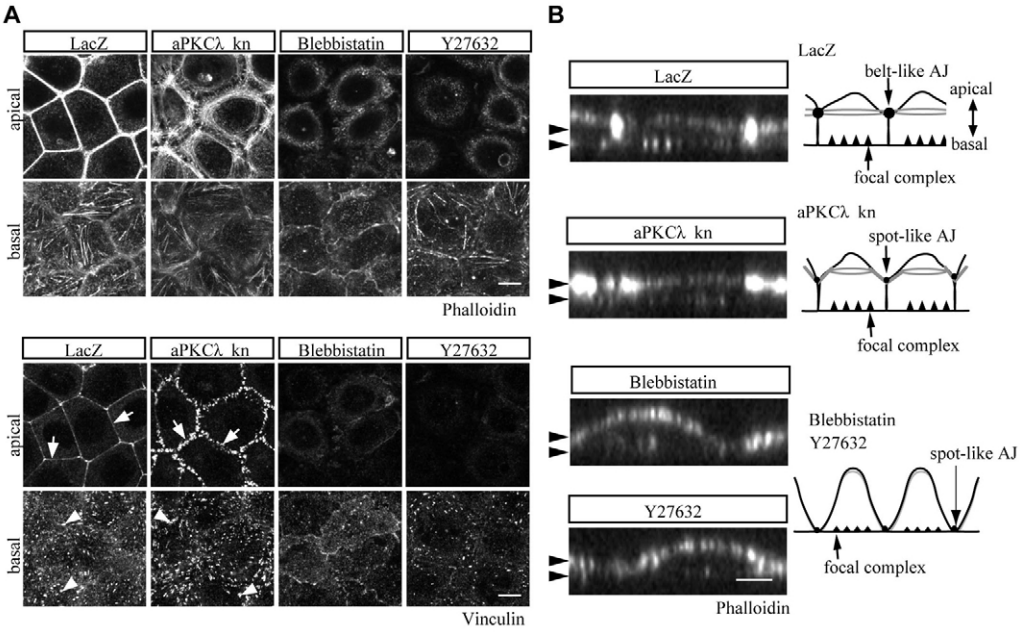

Fig. 3. Suppression of aPKC activity does not disrupt the polarized organization of vinculin-containing structures at regions of cell-cell and cell-substrate contact. (A) MTD1-A cells treated with the indicated adenovirus vectors or myosin inhibitors were subjected to a Ca^{2+} switch as described in the legend for Fig. 1, and were then immunostained with rhodamine-phalloidin (top panels) and an anti-vinculin antibody (bottom panels) at 6 hours after the Ca^{2+} switch. Single confocal sections at the basal planes (basal) and apical planes 2.5 μm upward from the basal planes (apical) are shown. The signal intensity of phalloidin staining in the basal planes was enhanced to a comparable level to that in the apical planes. Note that aPKCλ kn does not disrupt the polarized distribution of vinculin into the two distinct structures at apical cell-cell contacts (arrows) and basal cell-substrate contacts (arrowheads). By contrast, cells treated with myosin-II inhibitors exhibit vinculin staining in the same planes. (B) Reconstituted *xz* views of the cells demonstrated in A were presented for rhodamine-phalloidin staining. Arrowheads point to the apical and basal planes at which the confocal data were obtained. Scale bar: 10 μm.

Collectively, the present results indicate that the effect of aPKCλ kn on the development of belt-like AJs was not a result of inhibiting the myosin-II-dependent contractile force of the circumferential actin cables observed in the early stage of junctional development.

aPKCλ-kn-overexpressing cells exhibit myosin-II-dependent development of polarized F-actin organization and cuboidal cell shape

We previously reported that, despite incomplete formation of belt-like AJs, aPKCλ-kn-overexpressing cells develop a polarized columnar shape, in which the apical F-actin structures, such as the circumferential actin cables and radial actin fibers, are clearly separated from the basal stress fibers (Suzuki et al., 2002). Consistently, vinculin exhibited two kinds of discrete localization in aPKCλ-kn-overexpressing cells: at the apical cell-cell contacts (spot-like AJs) and at basal focal contacts (arrows and arrowheads, respectively, Fig. 3A,B). These findings were in sharp contrast to the effects of myosin-II inhibitors, which disrupt the increase in the lateral domain and development of a polarized organization of F-actin (Zhang et al., 2005). In these cases, vinculin staining at the cell-cell and cell-substrate contacts became significantly weaker, and were observed on the same focal plane at the basal side (Fig. 3A,B). Recently, Miyake et al. demonstrated that vinculin recruitment into cadherin-catenin complexes is tension dependent (Miyake et al., 2006). Furthermore, Zhang et al. demonstrated that myosin-II-based contraction is involved in the increase in the height of the lateral domain during epithelial-cell polarization (Zhang et al., 2005). Taken together, the present results suggest that aPKCλ-kn-overexpressing cells normally utilize myosin-II activity, at least in part, to develop their polarized F-actin organization and cuboidal cell shape. This is extremely consistent with the above results that show that aPKCλ kn did not interfere with the myosin-II activation observed at the early stage of junctional development. Nevertheless, cells lacking aPKC activity could not induce the transition of spot-like AJs into continuous AJs and TJs. Therefore, our results indicate the presence of a novel elementary process during the late stage of epithelial-junction development, in which aPKC activity is crucially required independently of myosin-II-dependent centripetal contraction of circumferential actin cables.

Centripetal contraction of the circumferential actin cables needs to be antagonized for use in epithelial-junction development

Next, we investigated what was lacking in aPKCλ-kn-overexpressing cells that was needed to promote epithelial-junction development. While considering this aspect, we noted that contraction of the circumferential actomyosin cables should conflict with expansion of the cables. Therefore, when cells become polarized, the myosin-II-mediated contractile force imposed on the circumferential actin cables needs to be counterbalanced by an antagonistic centrifugal force for use in junction development and cell polarization. If this does not occur, the contraction of the circumferential actomyosin cables would be detrimental to junction development. In fact, a recent study demonstrated that myosin-II-

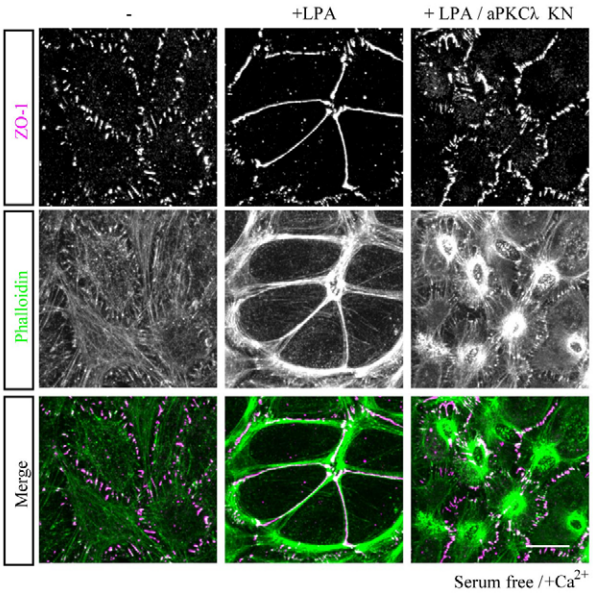

Fig. 4. Suppression of aPKC activity induces hyper-shrinkage of the circumferential actin cables during LPA-induced junction development in serum-starved MTD1-A cells. Confluent monolayers of MTD1-A cells infected with adenovirus vectors encoding β-galactosidase (– and +LPA) or aPKCλ kn were incubated in LC medium for 20 hours, with serum depletion from the medium during the last 1 hour, and then subjected to a Ca^{2+} switch by adding $CaCl_2$ with or without 10 μM LPA. The cells were stained with an anti-ZO-1 antibody (magenta in merged images) and phalloidin (green in merged images) at 2 hours after the Ca^{2+} switch. The images shown are projected views of *xy* confocal sections. The results did not change even when cells were stained at 6 hours after the Ca^{2+} switch (M.K. and A.S., unpublished). Note that serum starvation results in blockade of the development of dot-like AJs into belt-like AJs and this blockade is released by the addition of LPA. Overexpression of aPKCλ kn suppresses this LPA-induced junction development and induces hyper-shrinkage of F-actin. Scale bar: 10 μm.

dependent contraction of perijunctional actin belts plays a positive role in disassembly of epithelial cell-cell junctions when cadherin-mediated cell-cell adhesions are weakened by Ca^{2+} depletion (Ivanov et al., 2004). This indicates the possibility that aPKC regulates this putative outward force that is required for antagonizing the contractile force of the actomyosin cables, and thus contributes to epithelial-junction formation and polarization.

Consistent with this hypothesis, aPKCλ-kn-overexpressing cells sometimes showed hyper-shrinkage of the circumferential actin cables after a Ca^{2+} switch (supplementary material Fig. S3). This effect of aPKCλ kn was more conspicuous when junction development was acutely induced by lysophosphatidic acid (LPA) in serum-starved MTD1-A cells. During the course of the present study, we found that serum-starved MTD1-A cells could not develop continuous junction structures, even in the presence of Ca^{2+}, and terminated the junction development with spot-like AJ formation (Fig. 4; supplementary material Fig. S4) in a similar manner to myosin-II inhibitors. Consistent with the hypothesis that reduced myosin-II activity is one of the causes of the defects in serum-starved MTD1-A cells, addition of LPA, a physiological ligand for Rho activation, acutely induced a dramatic reorganization of F-actin, leading to the formation of circumferential actin cables, and restored normal junction development in a myosin-II-inhibitor-sensitive manner (Fig. 4; M.K. and A.S., unpublished). Again, aPKCλ kn inhibited this LPA-induced junction formation in serum-starved MTD1-A cells without suppressing the circumferential actin-cable formation (Fig. 4). Interestingly, and probably due to the acute myosin-II activation, most of the aPKCλ-kn-overexpressing cells exhibited hyper-shrinkage of the circumferential actomyosin cables, which were tethered to the dot-like AJs by radial actin fibers (Fig. 4). These results are consistent with the above hypothesis that aPKC activity is required to antagonize the centripetal contraction of actomyosin circumferential actin cables in the late phase of epithelial-junction development.

Time-lapse live imaging directly shows aPKC-dependent expansion of the circumferential actomyosin cables

To directly confirm the presence of antagonizing forces on the circumferential actomyosin cables and their roles in junction assembly, we performed time-lapse analyses of the Ca^{2+}-switch-induced F-actin reorganization using GFP-actin-expressing MTD1-A cells. First, we examined the Ca^{2+}-depletion-induced depolarization process of MTD1-A cells to directly confirm the presence of a centripetal contractile force on the perijunctional actin belts (Fig. 5A; see supplementary material Movie 1). In polarized cells, GFP-actin signals were observed on perijunctional actin belts as single lines at cell-cell borders (00:00). Upon Ca^{2+} depletion, the perijunctional actin belts in each cell abruptly shrank to small rings, which squeezed the cells at the basal side (00:09-00:30). These actin rings persisted for more than 20 hours after Ca^{2+} depletion and were initially tethered via prominent radially running actin fibers. In contrast to the radial actin fibers observed in junctional development, the distal tips of these actin fibers were positive for paxillin but not for E-cadherin, ZO-1 or aPKC, indicating their stress-fiber-like functions (Fig. 5B,C) (Suzuki et al., 2002). Interestingly, E-cadherin and ZO-1 were instead concentrated on the small actin rings, suggesting that these proteins were detached from cell-cell-contact regions by abrupt shrinkage of perijunctional actin belts (Fig. 5B) (Ivanov et al., 2004). Considering that perijunctional actin belts in polarized epithelial cells contain activated myosin II (Fig. 2C) and show a contractile nature in live imaging (see supplementary material Movie 2, 124-150 minutes) (Vaesi et al., 2002), the present results provide the first direct evidence for the notion that the myosin-II-mediated contractile force imposed on the perijunctional actin belt is counterbalanced by cell-cell adhesions mediated by E-cadherin, which hook up perijunctional actin belts of neighboring cells (Fig. 5D).

Next, we examined the dynamic actin reorganization during the cell-polarization process, as well as the effects of aPKC inhibition on this process (Fig. 6A,B). Complete depolarization of MTD1-A cells by prolonged Ca^{2+} depletion retarded the repolarization process to an extent that was unsuitable for live imaging. Therefore, we used cells subjected to shorter LC incubations; these cells retained small actin rings beneath the apical membrane (arrows) but not radially running actin fibers. In control cells expressing *lacZ*, these small actin rings gradually expanded after a Ca^{2+} switch, moved closer to cell-cell-contact regions (Fig. 6A, 00:00-01:00) and finally developed into perijunctional actin belts (Fig. 6A, arrowheads), as though the movie recording the depolarization process was rewound (see supplementary material Movie 2). Although not clearly discernible in every frame, radial actin fibers appeared to tether the rings to the cell-cell-contact region and their tense appearance suggested a role in the centrifugal expansion of the small actin rings. By contrast, expansion of the actin rings was severely impaired in aPKCλ-kn-overexpressing cells (Fig. 6B). Again, small actin rings were captured by tense radial actin fibers.

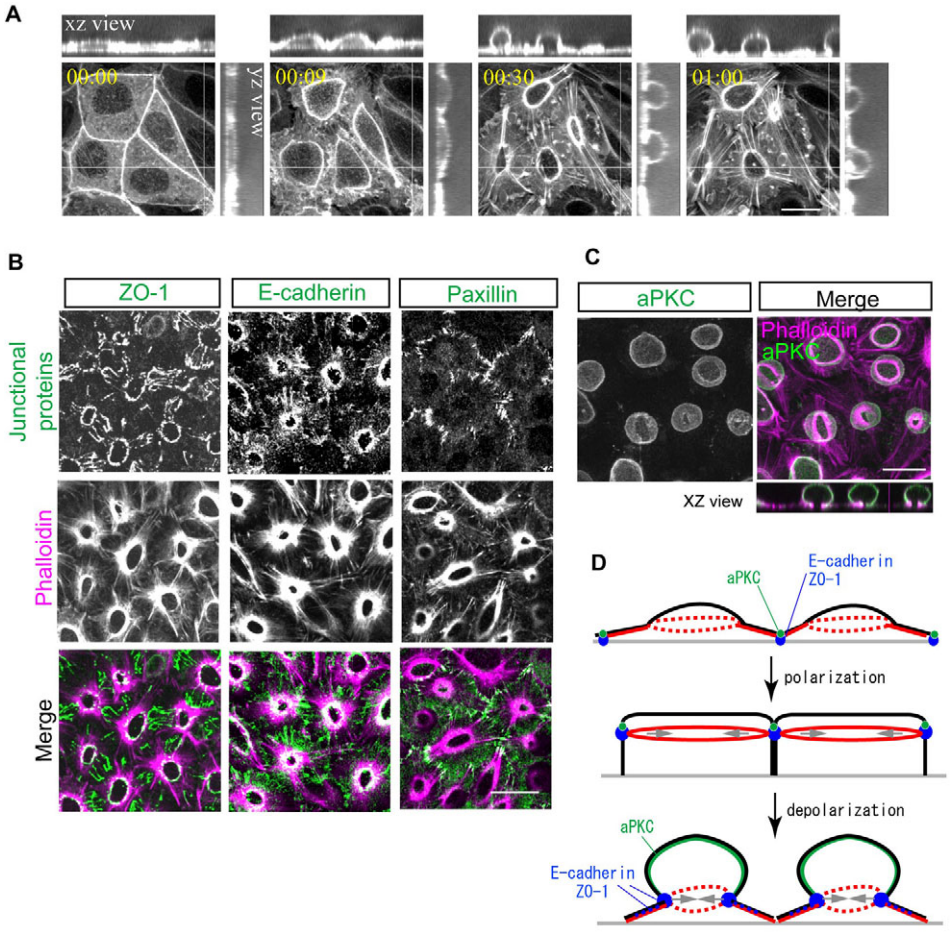

Fig. 5. Live-cell imaging of GFP-actin reveals the presence of a centripetal force imposed on the perijunctional actin belts. (A) Confluent monolayers of MTD1-A cells transfected with an adenovirus vector encoding GFP-actin were depolarized by Ca^{2+} depletion (00:00). Every 3 minutes, *z*-stack images were acquired at 1-μm intervals by time-lapse confocal microscopy (see supplementary material Movie 1). The images shown are still frames from the time-lapse data at the indicated times. Projected *xy* views as well as *z*-sectional views (*xz* and *yz* views) are presented. Note that the perijunctional actin belts rapidly shrink and squeeze the cells at their basal regions. The resultant small actin rings remain tethered to the cell peripheries by prominent radially running actin fibers. (B) Depolarized MTD1-A cells were fixed 45 minutes after Ca^{2+} depletion, and were double stained with the indicated antibodies (green in merged images) and rhodamine-phalloidin (magenta in merged images). Projected *xy* views of confocal sections are presented. Note that E-cadherin and ZO-1 predominantly localized on small actin rings but not at the tip of radially running actin fibers to which paxillin concentrated. (C) aPKC (green) localized on the apical surface of depolarized MTD1-A cells fixed as described in B. Scale bars: 10 μm. (D) Schematic illustrating the differences between polarizing and depolarizing MTD1-A cells. Note that the localizations of E-cadherin and ZO-1 (blue), and aPKC (green) are completely different between both states. Red lines illustrate F-actin organization.

However, they did not expand and instead shrank to very concentrated aggregates (see supplementary material Movie 3). In the present experimental condition, many actin rings that formed in aPKCλ-kn-overexpressing cells finally disassembled and disappeared.

As mentioned above, LPA-induced junction development proceeded more quickly in serum-starved MTD1-A cells than in cells induced by a Ca^{2+} switch. Thus, we used this experimental condition to examine the actin reorganization during repolarization of MTD1-A cells from the completely depolarized state (Fig. 7; see supplementary material Movies 4, 5). Probably due to its strong effects on activating the Rho-ROCK pathway, LPA acutely induced robust formation of radial actin fibers from the cell-cell-contact regions (Fig. 7A; arrows in Fig. 7B). Within 30 minutes, these radial fibers became associated with circumferential loose actin cables (arrowheads in Fig. 7B) derived from peripheral actin filaments. As the radial actin fibers became shorter and shorter in control cells expressing *lacZ*, the circumferential actin cables continued to expand and became perijunctional actin belts associated with cell-cell-contact regions (Fig. 7B, 00:30-01:45, arrowheads). aPKCλ-kn-overexpressing cells also developed radial actin fibers, which attached to loose circumferential actin cables and showed intense tensile stretch (see supplementary material Movie 5). However, the circumferential actin cables in these cells did not expand but rapidly showed asymmetric hyper-shrinkage and eventually formed small ring aggregates at the very apical regions out of focus (Fig. 7A, arrowheads; supplementary material Fig. S5). Taken together, these results are consistent with the notion that perijunctional actin belts are directly formed by expansion of the circumferential actin cables, and that aPKC activity is required for promoting this expansion against centripetal actomyosin contraction.

Circumferential actin cables might generate a driving force for their expansion by dragging radial actin fibers into them

Finally, to obtain insights into how the circumferential actin cables are expanded, we analyzed junction formation during wound healing of MTD1-A cells, which enabled us to dissect the actin dynamics much more clearly (Fig. 8A; supplementary material see Movie 6). Consistent with previous reports, radial actin fibers rapidly grew from nascent cell-cell contacts at the tips of the leading edges (Fig. 8A, arrowheads, 00:20) and eventually reached the intracellular circumferential actin cables, continuously showing centripetal (retrograde) flow (Fig. 8A, 00:35). Next, the radial actin fibers tagged onto the circumferential actin cables towards the cell-cell-contact region and accelerated wound closure (Fig. 8A,B; supplementary material Movie 6). Finally, the circumferential actin cables in the contacting cells moved closer to one another, became fused and developed into de novo perijunctional actin belts (Fig. 8C; see supplementary material Movie 7). Interestingly, during these processes, radial actin fibers gradually became aligned and finally fused with the attached circumferential actin cables without showing any obvious contractile movement (Fig. 8C). Taken together with the fact that radial actin fibers were free from myosin II (Fig. 2A,B), these results suggest the possibility that the circumferential actin cables drag radial actin fibers into them, thereby generating the driving force required for their own expansion. aPKC might affect

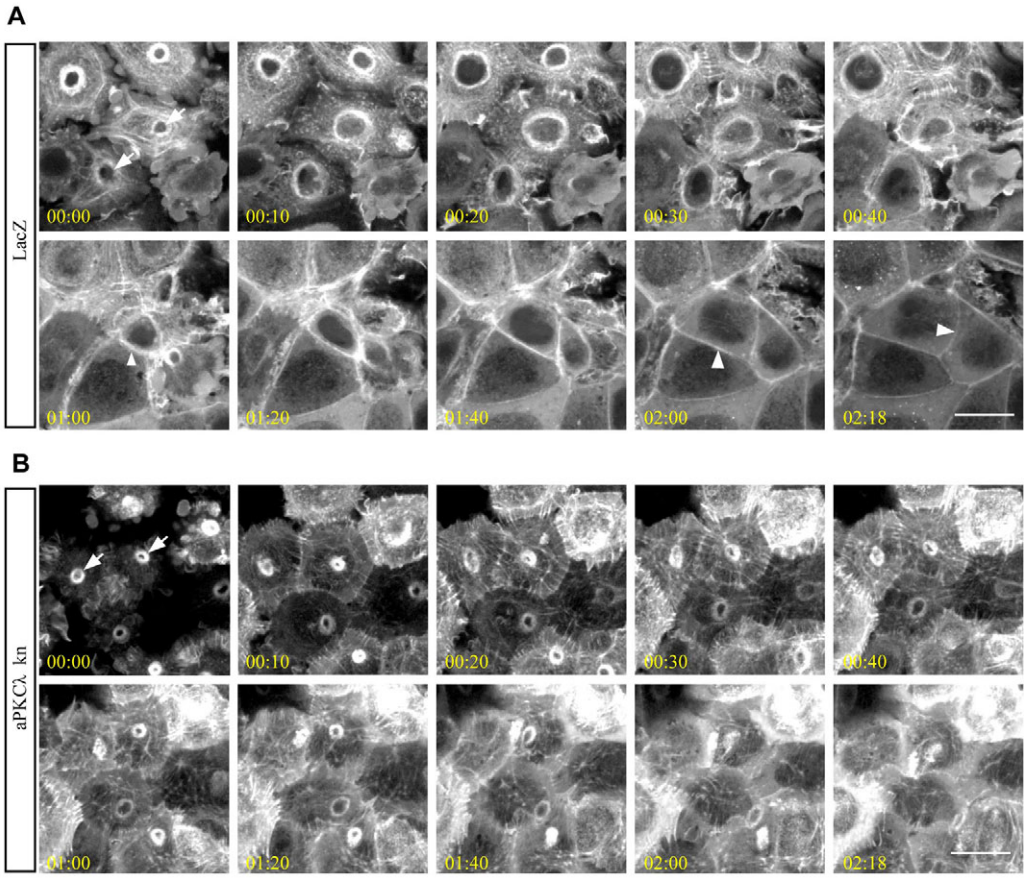

Fig. 6. Live-cell imaging of GFP-actin reveals the presence of a centrifugal force that expands the contractile circumferential actin cables in an aPKC-dependent manner during epithelial-cell polarization. (A,B) Confluent monolayers of MTD1-A cells transfected with an adenovirus vector encoding GFP-actin together with a vector encoding β-galactosidase (LacZ; A) or aPKCλ kn (B) were depolarized in LC medium for 20 hours and then subjected to a Ca^{2+} switch (00:00). *z*-stack images taken at 1-μm intervals for 4 μm were acquired by time-lapse confocal microscopy (see supplementary material Movies 2, 3). The images shown here are still frames from the time-lapse data at the indicated times. Projected *xy* views are presented. (A) Note that, in control cells, the actin-ring structures observed in depolarized cells are connected to cell-cell-contact regions and expand to form perijunctional actin belts as the cells become polarized. (B) In aPKCλ-kn-overexpressing cells, the rings are tethered by radial actin fibers but fail to expand and instead show hyper-shrinkage. Scale bars: 10 μm.

the expansion of the circumferential actin cables by promoting the drawing of radial actin fibers into the cables.

Discussion

Recent studies using the myosin-II-specific inhibitor blebbistatin have demonstrated the importance of myosin-II activity for the development of epithelium-specific junction structures and a columnar shape (Ivanov et al., 2005; Miyake et al., 2006; Zhang et al., 2005). These results are consistent with the commonly held idea that actomyosin contraction is important for the establishment of epithelial-cell polarity. However, because blebbistatin profoundly disrupts cell-cell-contact-induced F-actin reorganization, this inhibitor provides little information regarding how cells use actomyosin contraction for junction development. In the present study, we revealed that, despite its similar effect on junction development to that of myosin-II inhibitors, aPKC inhibition did not interfere with myosin-II activity in the early stage of junctional formation and allowed cells to form the apical circumferential actin cables required for maintaining their polarized columnar shape. These results revealed the presence of a novel elementary step in which aPKC promotes epithelial-junction development without interfering with the myosin-II-dependent centripetal contraction of circumferential actin cables. Importantly, by performing high-resolution live-cell imaging analyses of GFP-actin, we succeeded in observing for the first time that the contractile circumferential actin cables are centrifugally expanded by radial actin fibers and thus directly develop into perijunctional actin belts. Furthermore, aPKC inhibition specifically suppressed this crucial step of perijunctional actin-belt development. Taken together with the observation that aPKC inhibition frequently induced hyper-contraction of the circumferential actomyosin cables, we concluded that aPKC kinase activity is essential for cells to counterbalance the centripetal contraction of the circumferential actin cables and allow development of these cables into perijunctional actin belts (Fig. 9A).

The present results not only provide important clues regarding the molecular basis of how aPKC regulates epithelium-specific junction development, but also give rise to a novel concept that the contractile force of perijunctional actin belts needs to be counterbalanced for use in epithelial-junction development (if this does not occur, the contractile force of the circumferential actin cables is detrimental to cell adhesion). This idea effectively explains why myosin-II-dependent contraction is required for not only assembly but also disassembly of epithelial-junction structures (Ivanov et al., 2005; Ivanov et al., 2004). By contrast, the above idea seems inconsistent with an earlier model that suggested that the contraction of actomyosin cables is relieved in the vicinity of cell-cell contacts, and instead acts at cell-cell-contact-free regions of the membrane to expand the contact region laterally and bring the contacting cells together in a more compact manner (Fig. 9B) (Adams et al., 1998; Gloushankova et al., 1997; Krendel and Bonder, 1999; Yamada and Nelson, 2007). Although this model is based on observations that circumferential actomyosin cables disassembled near regions of epithelial cell-cell contact, we should be cautious because these results were obtained by analyzing asymmetrically formed cell-cell contacts; for example, two- or three-cell contacts observed under sparsely seeded conditions, or cell-cell contacts formed between leader cells observed in wound closure. As far as

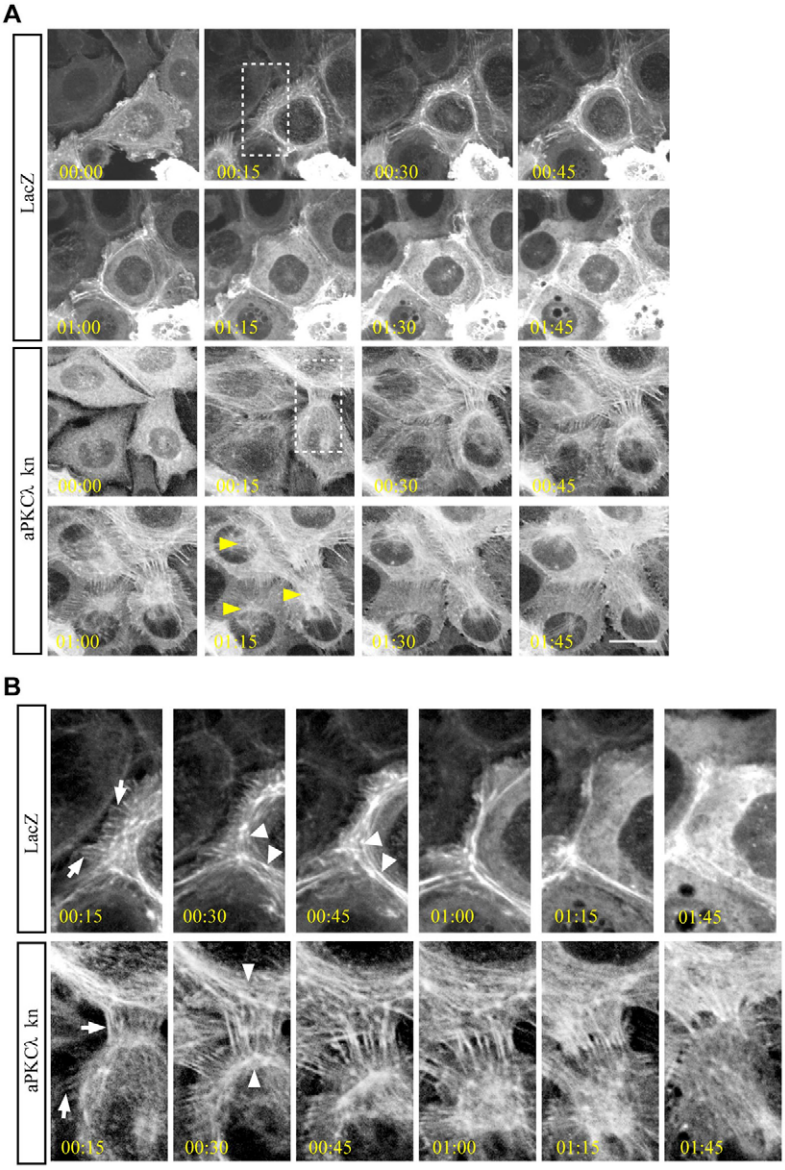

Fig. 7. aPKCλ kn does not affect the formation of the radial actin fibers that is rapidly induced by LPA in serum-depleted MTD1-A cells. (A) Subconfluent MTD1-A cells expressing GFP-actin together with β-galactosidase (LacZ) or aPKCλ kn were depolarized in LC medium for 48 hours and subjected to serum starvation as described in the legend for Fig. 4. $CaCl_2$ and LPA were simultaneously added to the cells at time 0, and time-lapse images were acquired by confocal microscopy (see supplementary material Movies 4, 5). The images shown are still-frames (projected *xy* views of intermediate sections) from the time-lapse data at the indicated times. (B) Enlarged views corresponding to the boxed regions in A. Scale bar: 10 μm.

we could examine, it is not easily applicable to the polarization process of confluent epithelial cells that develop cell-cell contacts rather symmetrically and essentially lack cell-cell-contact-free regions of the membrane. We observed in our wound-healing experiments that the association of radial actin fibers impaired the integrity of the circumferential actin cables and sometimes caused complete disassembly of the cables in the vicinity of cell-cell contacts, especially when their association occurred at very restricted regions (see supplementary material Movie 8). In these cases, the ends of the fragmented circumferential actin cables of each contacting cell fused to form arc-like cables at the edges of the contact-free surfaces and appeared to shrink to minimize the cell-cell-contact-free area in a purse-string manner (Krendel and Bonder, 1999). However, even in wound healing, the circumferential actin cables did not always disassemble completely, but often directly developed into strong perijunctional actin belts (Fig. 7A,B: see supplementary material Movie 9). Also, we did not observe the complete disappearance of circumferential actin cables during the polarization process of confluent MTD1-A cells, in which multiple associations of radial actin fibers with the circumferential actin cables occurred almost simultaneously. Taken together, we propose that, at least during the polarization process of confluent epithelial cells, the contractile force of the circumferential actin cables is not diminished but is counterbalanced by an antagonistic centrifugal force transmitted from the radial actin fibers in order to be efficiently used for the development of continuous junction structures (Fig. 9A).

The present results also provided a novel idea that aPKC kinase activity, which is thought to be activated upon initial cell-cell adhesion (Suzuki et al., 2002), contributes to epithelial-cell polarity by coupling the centripetal contractile forces of the circumferential actomyosin cables with the development of epithelium-specific junction structures. aPKC inhibition did not affect the formation of radial actin fibers or their linkage with the circumferential actin cables (Fig. 7; see supplementary material Movie 5). Therefore, the activation of aPKC appears to be required for the generation of an outward-pulling force imposed on the circumferential actin cables through radial actin fibers. We have not been able to ascertain the precise nature of this force or the molecular mechanism by which aPKC affects this force generation. However, the present results suggested that the entanglement and dragging of radial actin fibers into the circumferential actin cables provided the driving force required for the centrifugal expansion of the circumferential actomyosin cables themselves (Fig. 9C). In this model, we postulate that the entangled radial actin fibers are dragged into the circumferential actin by the myosin-II-dependent centripetal contraction of the circumferential actin cables. Therefore, this hypothesis is based on an apparently self-contradictory idea that, by contracting centripetally, the circumferential actomyosin cables generate the centrifugal force required for their outward expansion. That is, the more the circumferential actin cables drag radial fibers within themselves, the more these cables are subjected to the outward force. Although we confirmed that aPKC kn did not affect MLC2 monophosphorylation (Fig. 2), aPKC might phosphorylate the myosin heavy chain and affecting its assembly (Even-Faitelson and Ravid, 2006). We also cannot exclude the possibility that aPKC activates myosin-II activity by regulating the diphosphorylation of MLC2 (see supplementary material Fig. S2), although the upregulation of this phosphorylation appeared to occur too late to affect circumferential actin-cable expansion. By contrast, there remains another possibility that aPKC regulates actin polymerization at spot-like AJs and thereby promotes

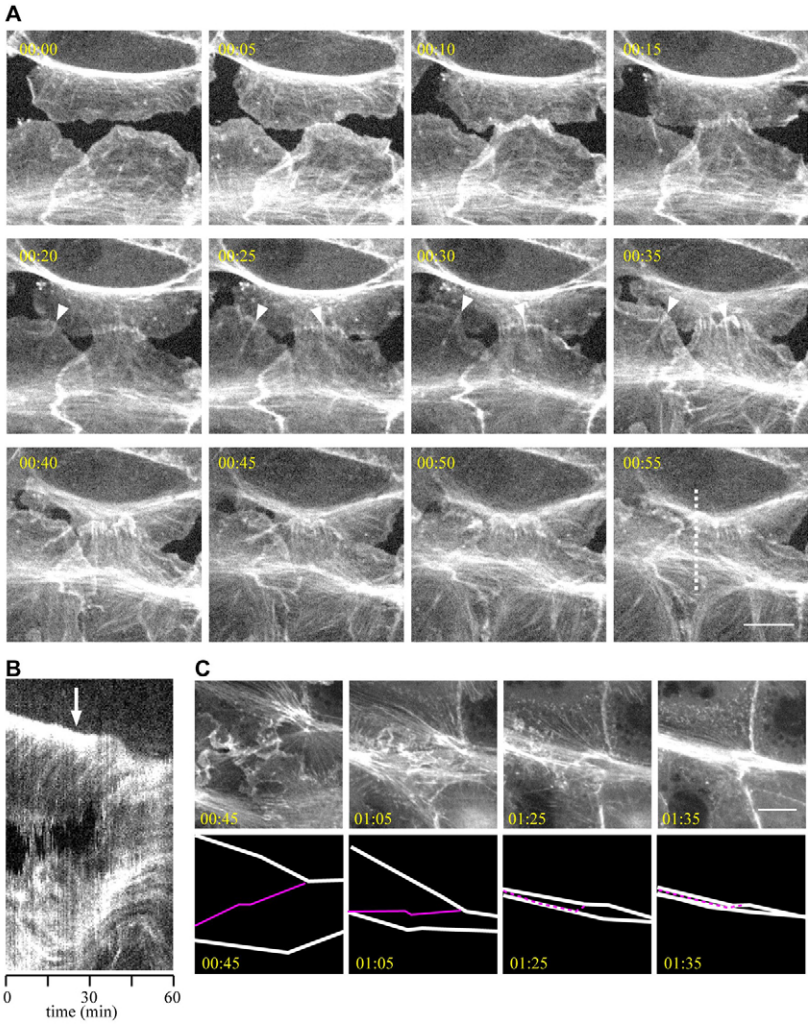

Fig. 8. GFP-actin dynamics during wound healing of MTD1-A cells. (A) Confluent monolayers of MTD1-A cells stably expressing GFP-actin were scratched with a needle (18 gauge) after a brief incubation in PBS. Time-lapse images of GFP-actin (single confocal sections) were acquired by confocal microscopy at an appropriate time after wounding (see supplementary material Movie 6). The images shown are still-frames from the time-lapse data at the indicated times. Note that rapid actin polymerization occurs at the tips of the leading edges immediately after the initial cell-cell contacts (arrowheads), and the resultant radial actin fibers tag the circumferential actin cables when they come into contact (00:35). (B) The images in A were subjected to kymograph analysis to monitor the changes in the distance between the two circumferential actin cables in contacting cells along the broken line. Arrow, indicates the time point when radial actin fibers reached the intracellular circumferential actin cables. (C) GFP-actin dynamics at the late stage of wound healing. Note that the radial actin fibers (traced by magenta lines in the bottom panels) are aligned and fused with the corresponding circumferential actin cables (illustrated by white lines in the bottom panels) (see supplementary material Movie 7). Scale bars: 10 μm.

effective dragging of the radial actin fibers indirectly, because aPKC was mainly localized at the spot-like AJs immediately after the initial cell-cell contacts (Fig. 9A, red circles), and because epithelial junction formation has been shown to depend on nucleation of actin filaments (Ivanov et al., 2005). aPKC has also been shown to phosphorylate several polarity proteins, such as PAR-1 (Suzuki et al., 2004), PAR-3 (Nagai-Tamai et al., 2002) and Lgl (Yamanaka et al., 2003), during the epithelial-cell polarization process. Therefore, we also need to examine possibilities that aPKC indirectly affects myosin-II activity through the phosphorylation of these polarity proteins; especially Lgl, which has been shown to inhibit myosin-II activity in *Drosophila* embryogenesis (Munro et al., 2004). Although phenomenological, the present study provides important clues to elucidate the molecular targets of aPKC that are crucially involved in epithelium-specific junction development. Future studies are required to clarify the molecular basis underlying this novel function of aPKC.

Materials and Methods

Cell culture

MTD1-A cells, a polarized epithelial cell line from a mouse mammary tumor (Enami et al., 1984; Hirose et al., 2002), were cultured in Dulbecco's modified Eagle's medium (DMEM) supplemented with 10% fetal bovine serum (FBS). When subjected to a Ca^{2+} switch, cells were incubated in LC medium containing 5% FBS and 3 μM Ca^{2+} for more than 40 hours, and were then switched to a normal Ca^{2+} (NC) growth medium containing 1.8 mM $CaCl_2$ (Gumbiner and Simons, 1986; Stuart et al., 1994). At appropriate times after the Ca^{2+} switch, cells were processed for immunofluorescence analysis. For brief serum starvation, cells depolarized in LC medium were switched to serum-depleted LC medium for 1 hour, before $CaCl_2$ was added to a final concentration of 1.8 mM to induce the formation of cell-cell contacts. To establish MTD1-A clones that stably expressed GFP-actin, cells were transfected with a GFP-actin expression vector (Clontech) in OPTI-MEM using Lipofectamine 2000 (Invitrogen) and were selected in growth medium containing 400 μg/ml of G418 for 2 weeks.

Drug treatment

To inhibit myosin-II activity, confluent MTD1-A cells grown in LC medium for ~40 hours were pre-treated with 100 μM blebbistatin (Calbiochem), 20 μM Y27632 (Calbiochem) or vehicle as a control for 1 hour, and then transferred to NC medium containing the same drugs to induce cell-cell-contact formation. To induce belt-like AJ formation in serum-starved MTD1-A cells, 10 μM LPA (Sigma) was added simultaneously or at 2 hours after the Ca^{2+} addition.

Adenovirus infection

The adenovirus expression vectors encoding *lacZ* and aPKCλ kn, a dominant-negative mutant of aPKCλ, were described previously (Ebnet et al., 2001). MTD1-A cells were seeded on coverslips at a density of 1×10^5 cells/cm^2, cultured for 2-3 days, incubated with the appropriate virus solution (1×10^7 pfu/ml) in LC medium overnight and then subjected to a Ca^{2+} switch. We confirmed that this infection procedure resulted in ~100% expression of the ectopic proteins (M.K. and A.S., unpublished). For time-lapse imaging of actin dynamics, an adenovirus expression vector encoding GFP-actin (Furuyashiki et al., 2002) was simultaneously transformed with *lacZ* or aPKCλ kn.

RNA interference

Synthetic RNA oligonucleotide duplexes with 3′-dTdT overhangs based on the sequences 5′-GGUUGUUUUUUGUCAUAGA-3 for mouse *aPKCλ* and 5′-GGAAAAGUUAGCGUGUAAU-3′ for mouse *aPKCζ* were purchased from Ambion. The sequence 5′-AATTCTCCGAACGTGTCACGT-3′ was used for control

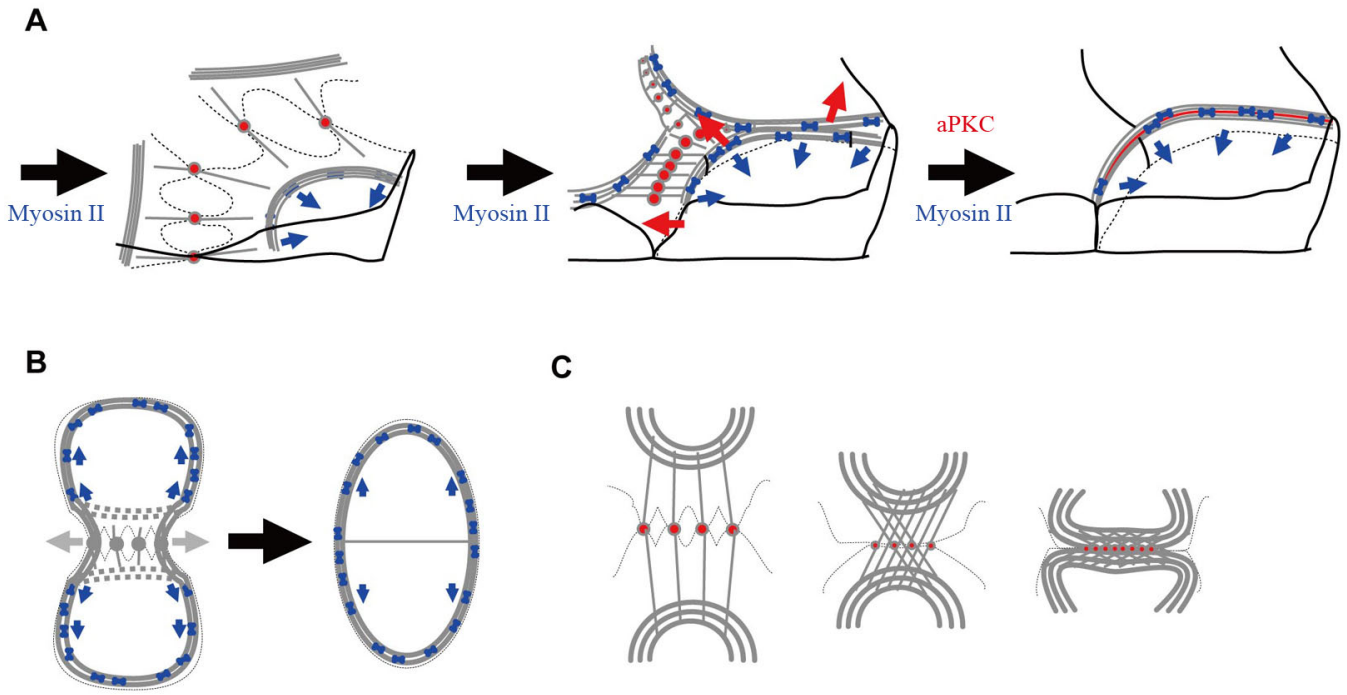

Fig. 9. New model for the role of the circumferential actin cables in junction development of confluent epithelial cells. (A) Newly proposed model for the role of the contraction of the circumferential actin cables in epithelial-junction development. In this model, the centripetal contractile force of the circumferential actomyosin cable (blue arrows) is counterbalanced by an aPKC-dependent putative centrifugal force (red arrows), such that it can be used for the development of continuous junction structures. Grey lines and circles, F-actin structures; dumb-bell-like symbols, myosin II; red circles, aPKC. (B) A previously published model suggesting that actomyosin contraction works at cell-cell-contact-free regions of the cell membrane in order to be used for lateral expansion of cell-cell contact regions (Adams et al., 1998; Gloushankova et al., 1997; Krendel and Bonder, 1999; Yamada and Nelson, 2007). (C) A possible mechanism by which the radial actin fibers are integrated into the circumferential actin cables. Grey lines and circles, F-actin structures; red circles, aPKC.

experiments. MTD1-A cells (2×10^6 cells) were transfected with each duplex (4 μg) by electroporation, according to the manufacturer's instructions (Amaxa). To obtain high knockdown efficiency, cells were harvested the next day and subjected to a second electroporation with the same RNA duplexes.

Antibodies

The following monoclonal and polyclonal antibodies (mAb and pAb, respectively) were used: anti-ZO-1 mAb (clone ZO1-1A12, 33-9100; Zymed Laboratories); anti-ZO-1 pAb (MAB1520; Chemicon); anti-E-cadherin mAb (clone DECMA-1, U3254; Sigma); anti-α-catenin mAb (clone 5, 610193; Becton Dickinson); anti-β-catenin mAb (clone 14, 610153; Becton Dickinson); anti-myosin-IIA pAb (M8064; Sigma); anti-myosin-IIB pAb (M7939; Sigma); anti-α-actinin-1 mAb (clone BM75.2, A5044; Sigma); anti-vinculin mAb (clone hVIN-1, V9131; Sigma); anti-paxillin mAb (clone 349, 610051; Becton Dickinson); anti-α-tubulin mAb (clone DM1A, T6199; Sigma); anti-GAPDH mAb (clone 6C2, ab8245; Abcam); anti-phosho-MLC2 (Ser19) mAb (3675; Cell Signaling); anti-phosho-MLC2 (Thr18/Ser19) pAb (3674; Cell Signaling); and anti-aPKCζ pAb (C20; Santa Cruz Biotechnology). The anti-myosin-IIA and -IIB pAbs were mixed for staining of myosin II in MTD1-A cells. An anti-aPKCι (human aPKCλ) mAb (clone 23, 610176; Becton Dickinson) was used for specific detection of aPKCλ/ι in western blot analyses.

Immunofluorescence analysis

Cells seeded on coverslips were fixed with 1.5% paraformaldehyde in PBS for 12 minutes at room temperature, washed twice with PBS and permeabilized with 0.5% Triton X-100 in PBS for 10 minutes at room temperature. The cells were then washed and soaked in blocking solution (PBS containing 10% calf serum) for 30 minutes at room temperature before incubation overnight at 4°C with an appropriate primary antibody diluted in 10 mM Tris-HCl (pH 7.5) containing 150 mM NaCl, 0.01% (v/v) Tween 20 and 0.1% (w/v) BSA. The secondary antibodies used were Alexa-488-conjugated goat anti-rabbit IgG and Alexa-568-conjugated goat anti-mouse IgG (Molecular Probes). To stain F-actin, rhodamine-phalloidin (Molecular Probes) was used in place of a secondary antibody. Coverslips were mounted using PBS (pH 8.5) containing 50% (w/v) glycerol and 0.01% (w/v) p-phenylenediamine. Confocal microscopy images were obtained using a Leica DM IRE2 microscopy system equipped with a spinning-disc confocal system, CSU10 (Yokogawa) or a Zeiss LSM microscopy system. In some cases, cells were subjected to time-lapse imaging using the Leica DM IRE2 microscopy system as described below.

Time-lapse imaging

Cells were placed in a closed heat-controlled chamber (Leica) with a CO_2 supply system (Tokken) on a Leica IRB2 inverted microscope equipped with an automated filter wheel (Ludl Electronic Products), CSU10 (Yokogawa) and an Orca II CCD camera (Hamamatsu Photonics). Video microscopy was performed with a 63× plan apochromatic objective with a numerical aperture of 1.4. GFP was excited with an Ar/Kr laser through a GFP excitation filter. Time-lapse images were acquired with the MetaMorph software (Molecular Devices), and the movies were edited using ImageJ (NIH). For bright visualization, the contrast of each frame in each movie was enhanced using ImageJ software.

We would like to thank Haruhiko Bito (Tokyo University, Japan) for the generous gift of the adenovirus expression vector encoding GFP-actin; and Shigenobu Yonemura (RIKEN, Japan), Yuko Kiyosue (Kan-Research Laboratory, Japan) and our laboratory members for helpful discussions. This work was supported by Grants from the Ministry of Education, Culture, Sports, Science and Technology of Japan (S.O.), and the Japanese Society for the Promotion of Science (S.O., M.K.).

References

Adams, C. L., Nelson, W. J. and Smith, S. J. (1996). Quantitative analysis of cadherin-catenin-actin reorganization during development of cell-cell adhesion. *J. Cell Biol.* **135**, 1899-1911.

Adams, C. L., Chen, Y. T., Smith, S. J. and Nelson, W. J. (1998). Mechanisms of epithelial cell-cell adhesion and cell compaction revealed by high-resolution tracking of E-cadherin-green fluorescent protein. *J. Cell Biol.* **142**, 1105-1119.

Barros, C. S., Phelps, C. B. and Brand, A. H. (2003). Drosophila nonmuscle myosin II promotes the asymmetric segregation of cell fate determinants by cortical exclusion rather than active transport. *Dev. Cell* **5**, 829-840.

Chen, X. and Macara, I. G. (2005). Par-3 controls tight junction assembly through the Rac exchange factor Tiam1. *Nat. Cell Biol.* **7**, 262-269.

Ebnet, K., Suzuki, A., Horikoshi, Y., Hirose, T., Meyer Zu Brickwedde, M. K., Ohno, S. and Vestweber, D. (2001). The cell polarity protein ASIP/PAR-3 directly associates with junctional adhesion molecule (JAM). *EMBO J.* **20**, 3738-3748.

Enami, J., Enami, S. and Koga, M. (1984). Isolation of an insulin-responsive preadipose cell line and a mammary tumor virus-producing, dome-forming epithelial cell line from a mouse mammary tumor. *Dev. Growth Differ.* **26**, 223-234.

Even-Faitelson, L. and Ravid, S. (2006). PAK1 and aPKCzeta regulate myosin II-B phosphorylation: a novel signaling pathway regulating filament assembly. *Mol. Biol. Cell* **17**, 2869-2881.

Furuyashiki, T., Arakawa, Y., Takemoto-Kimura, S., Bito, H. and Narumiya, S. (2002). Multiple spatiotemporal modes of actin reorganization by NMDA receptors and voltage-gated Ca^{2+} channels. *Proc. Natl. Acad. Sci. USA* **99**, 14458-14463.

Gloushankova, N. A., Alieva, N. A., Krendel, M. F., Bonder, E. M., Feder, H. H., Vasiliev, J. M. and Gelfand, I. M. (1997). Cell-cell contact changes the dynamics of lamellar activity in nontransformed epitheliocytes but not in their ras-transformed descendants. *Proc. Natl. Acad. Sci. USA* **94**, 879-883.

Gumbiner, B. and Simons, K. (1986). A functional assay for proteins involved in establishing an epithelial occluding barrier: identification of a uvomorulin-like polypeptide. *J. Cell Biol.* **102**, 457-468.

Hirose, T., Izumi, Y., Nagashima, Y., Tamai-Nagai, Y., Kurihara, H., Sakai, T., Suzuki, Y., Yamanaka, T., Suzuki, A., Mizuno, K. et al. (2002). Involvement of ASIP/PAR-3 in the promotion of epithelial tight junction formation. *J. Cell Sci.* **115**, 2485-2495.

Ivanov, A. I., McCall, I. C., Parkos, C. A. and Nusrat, A. (2004). Role for actin filament turnover and a myosin II motor in cytoskeleton-driven disassembly of the epithelial apical junctional complex. *Mol. Biol. Cell* **15**, 2639-2651.

Ivanov, A. I., Hunt, D., Utech, M., Nusrat, A. and Parkos, C. A. (2005). Differential roles for actin polymerization and a myosin II motor in assembly of the epithelial apical junctional complex. *Mol. Biol. Cell* **16**, 2636-2650.

Ivanov, A. I., Bachar, M., Babbin, B. A., Adelstein, R. S., Nusrat, A. and Parkos, C. A. (2007). A unique role for nonmuscle myosin heavy chain IIA in regulation of epithelial apical junctions. *PLoS ONE* **2**, e658.

Knust, E. and Bossinger, O. (2002). Composition and formation of intercellular junctions in epithelial cells. *Science* **298**, 1955-1959.

Krendel, M. F. and Bonder, E. M. (1999). Analysis of actin filament bundle dynamics during contact formation in live epithelial cells. *Cell Motil. Cytoskeleton* **43**, 296-309.

Macara, I. G. (2004). Parsing the polarity code. *Nat. Rev. Mol. Cell Biol.* **5**, 220-231.

Mege, R. M., Gavard, J. and Lambert, M. (2006). Regulation of cell-cell junctions by the cytoskeleton. *Curr. Opin. Cell Biol.* **18**, 541-548.

Miyake, Y., Inoue, N., Nishimura, K., Kinoshita, N., Hosoya, H. and Yonemura, S. (2006). Actomyosin tension is required for correct recruitment of adherens junction components and zonula occludens formation. *Exp. Cell Res.* **312**, 1637-1650.

Munro, E., Nance, J. and Priess, J. R. (2004). Cortical flows powered by asymmetrical contraction transport PAR proteins to establish and maintain anterior-posterior polarity in the early C. elegans embryo. *Dev. Cell* **7**, 413-424.

Nagai-Tamai, Y., Mizuno, K., Hirose, T., Suzuki, A. and Ohno, S. (2002). Regulated protein-protein interaction between aPKC and PAR-3 plays an essential role in the polarization of epithelial cells. *Genes Cells* **7**, 1161-1171.

Narumiya, S., Ishizaki, T. and Uehata, M. (2000). Use and properties of ROCK-specific inhibitor Y-27632. *Meth. Enzymol.* **325**, 273-284.

Nelson, W. J. (2003). Adaptation of core mechanisms to generate cell polarity. *Nature* **422**, 766-774.

Shewan, A. M., Maddugoda, M., Kraemer, A., Stehbens, S. J., Verma, S., Kovacs, E. M. and Yap, A. S. (2005). Myosin 2 is a key Rho kinase target necessary for the local concentration of E-cadherin at cell-cell contacts. *Mol. Biol. Cell* **16**, 4531-4542.

Straight, A. F., Cheung, A., Limouze, J., Chen, I., Westwood, N. J., Sellers, J. R. and Mitchison, T. J. (2003). Dissecting temporal and spatial control of cytokinesis with a myosin II inhibitor. *Science* **299**, 1743-1747.

Stuart, R. O., Sun, A., Panichas, M., Hebert, S. C., Brenner, B. M. and Nigam, S. K. (1994). Critical role for intracellular calcium in tight junction biogenesis. *J. Cell Physiol.* **159**, 423-433.

Suzuki, A. and Ohno, S. (2006). The PAR-aPKC system: lessons in polarity. *J. Cell Sci.* **119**, 979-987.

Suzuki, A., Yamanaka, T., Hirose, T., Manabe, N., Mizuno, K., Shimizu, M., Akimoto, K., Izumi, Y., Ohnishi, T. and Ohno, S. (2001). Atypical protein kinase C is involved in the evolutionarily conserved par protein complex and plays a critical role in establishing epithelia-specific junctional structures. *J. Cell Biol.* **152**, 1183-1196.

Suzuki, A., Ishiyama, C., Hashiba, K., Shimizu, M., Ebnet, K. and Ohno, S. (2002). aPKC kinase activity is required for the asymmetric differentiation of the premature junctional complex during epithelial cell polarization. *J. Cell Sci.* **115**, 3565-3573.

Suzuki, A., Hirata, M., Kamimura, K., Maniwa, R., Yamanaka, T., Mizuno, K., Kishikawa, M., Hirose, H., Amano, Y., Izumi, N. et al. (2004). aPKC acts upstream of PAR-1b in both the establishment and maintenance of mammalian epithelial polarity. *Curr. Biol.* **14**, 1425-1435.

Tsukita, S., Nagafuchi, A. and Yonemura, S. (1992). Molecular linkage between cadherins and actin filaments in cell-cell adherens junctions. *Curr. Opin. Cell Biol.* **4**, 834-839.

Vaezi, A., Bauer, C., Vasioukhin, V. and Fuchs, E. (2002). Actin cable dynamics and Rho/Rock orchestrate a polarized cytoskeletal architecture in the early steps of assembling a stratified epithelium. *Dev. Cell* **3**, 367-381.

Vasioukhin, V., Bauer, C., Yin, M. and Fuchs, E. (2000). Directed actin polymerization is the driving force for epithelial cell-cell adhesion. *Cell* **100**, 209-219.

Yamada, S. and Nelson, W. J. (2007). Localized zones of Rho and Rac activities drive initiation and expansion of epithelial cell-cell adhesion. *J. Cell Biol.* **178**, 517-527.

Yamanaka, T., Horikoshi, Y., Sugiyama, Y., Ishiyama, C., Suzuki, A., Hirose, T., Iwamatsu, A., Shinohara, A. and Ohno, S. (2003). Mammalian Lgl forms a protein complex with PAR-6 and aPKC independently of PAR-3 to regulate epithelial cell polarity. *Curr. Biol.* **13**, 734-743.

Yeaman, C., Grindstaff, K. K. and Nelson, W. J. (1999). New perspectives on mechanisms involved in generating epithelial cell polarity. *Physiol. Rev.* **79**, 73-98.

Yonemura, S., Itoh, M., Nagafuchi, A. and Tsukita, S. (1995). Cell-to-cell adherens junction formation and actin filament organization: similarities and differences between non-polarized fibroblasts and polarized epithelial cells. *J. Cell Sci.* **108**, 127-142.

Zhang, J., Betson, M., Erasmus, J., Zeikos, K., Bailly, M., Cramer, L. P. and Braga, V. M. (2005). Actin at cell-cell junctions is composed of two dynamic and functional populations. *J. Cell Sci.* **118**, 5549-5562.